

Disproportionate increase in freshwater methane emissions induced by experimental warming

Authors: Yizhu Zhu¹, Kevin J Purdy², Özge Eyice¹, Lidong Shen^{1,3}, Sarah F Harpenslager^{1,4}, Gabriel Yvon-Durocher⁵, Alex J. Dumbrell⁶, Mark Trimmer^{1*}

Affiliations:

¹School of Biological and Chemical Sciences, Queen Mary University of London, London, E1 4NS, UK.

²School of Life Sciences, University of Warwick, Coventry, CV4 7AL, UK.

³Institute of Ecology, School of Applied Meteorology, Nanjing University of Information Science and Technology, Nanjing 210044, China.

⁴Leibniz Institute of Freshwater Ecology and Inland Fisheries (IGB), Department of Ecosystem Research, 12587, Berlin, Germany.

⁵Environment and Sustainability Institute, University of Exeter, Penryn Campus, Penryn, Cornwall, TR10 9FE, UK.

⁶School of Life Sciences, University of Essex, Colchester, Essex, U.K. CO4 3SQ.

*Correspondence to: Mark Trimmer m.trimmer@qmul.ac.uk

Words in main text: 2148 and words in Methods: 3374

Words in introductory paragraph: 150

Figures: 5 and Extended data figures: 3

References in main text: 37 and references in Methods only: 19

Main text:

Net emissions of the potent greenhouse gas methane from ecosystems represent the balance between microbial methane production (methanogenesis) and oxidation (methanotrophy), each with different sensitivities to temperature. How this balance will be altered by long term global warming, especially in freshwaters that are major methane sources, remains unknown. Here we show that experimental warming of artificial ponds over 11 years drives a disproportionate increase in methanogenesis over methanotrophy that increases the warming potential of the gases they emit. Increased methane emissions far exceed temperature-based predictions, driven by shifts in the methanogen community under warming, while the methanotroph community was conserved. Our experimentally induced increase in methane emissions from artificial ponds is, in part, reflected globally as a disproportionate increase in the capacity of naturally warmer ecosystems to emit more methane. Our findings indicate that as Earth warms, natural ecosystems will emit disproportionately more methane in a positive feedback warming loop.

Methane makes a large contribution to climate change and methane concentrations are increasing in the atmosphere^{1,2}. A significant proportion (~42% of all natural and anthropogenic sources) of methane is emitted from freshwaters (wetlands, lakes and rivers) that make a disproportionately large contribution to the global methane budget for their comparatively modest sizes^{3,4}. Methane production by methanogens and its oxidation by methanotrophs drive the biological methane cycle, with the balance between the two regulating net methane emissions⁵. Methanogenesis is very sensitive to temperature⁶, e.g. an increase of 10°C would drive a 4.0-fold increase in methane production^{7,8}, while, in contrast, methanotrophy⁹, being more strongly substrate limited, is less sensitive to temperature¹⁰. Due to these different physiological responses to temperature, long-term warming might alter the structure of methanogen and methanotroph communities, disturbing the balance between the two processes and ultimately increasing methane emissions^{11,12}.

Linking microbial community structure to ecosystem-level processes is a major theoretical challenge¹³. Therefore, measuring microbial community characteristics such as functional diversity^{12,14}, gene abundance¹⁵, growth efficiency¹⁶ and thermodynamic constraints¹⁷ is essential to determine how microbial community structure influences ecosystem-level processes¹³. This need is particularly acute at the long-term time-scale in the methane cycle as previous investigations into the effect of warming on methanogenesis and methanotrophy were typically limited to less than 1 year which may have masked the effects of any shifts in the microbial communities^{12,18,19}. Key unanswered questions under current climate warming scenarios remain: **1**, does long-term warming (>10 years) alter the balance between methanogenesis and methanotrophy; and **2**, how do any changes in the methane-related microbial communities affect net methane emissions?

We answered these questions by studying the long-term effects of warming on freshwater ecosystem-level methane cycling in 20 well-established, artificial ponds^{20,21}, half of which have been heated to 4°C above ambient since September 2006. Each pond is 1.8m wide, has a surface area of 2.5m² and approximately 50cm of water over 10cm of sandy sediments (Extended Data Figure 1). After 11 years of warming, frequent measurements (three times daily) revealed an ongoing divergence in methane emissions from the surface of the ponds to the atmosphere between our warmed and ambient ponds (Fig. 1a and Extended Data Fig. 2). Annual methane emissions are now 2.4-fold higher under warming and far in excess of the 1.7-fold increase predicted (*see* equation 2) through a simple physiological response to higher temperatures alone^{7,8}. Here methane emissions are dominated by diffusion (98.8%) rather than ebullition (1.2%)²², probably because of the relatively shallow sediments in our ponds (~ 10 cm) but the magnitude of ebullition is similarly amplified under warming (Supplementary Fig. 1). Even though the ponds are net sinks for CO₂^{20,21}, the ratio of CH₄ to CO₂ emitted at night has also increased by 1.8-fold under warming, increasing the global warming potential (GWP) of the carbon-gases emitted overall (Fig. 1b)². These long-term observations underline the potential of climate-warming to continually amplify methane emissions from freshwaters; a prediction that is supported by a meta-analysis showing an

increase in the capacity of wetlands, grasslands and soils to emit methane in regions with higher annual average temperatures (Fig. 1c and *see* Supplementary Table 1 for sites included) and from observations of increased methane emissions, driven by a fundamental change in the ecosystem, along a natural gradient of thawing permafrost²³. These observations clearly show that the methane cycle does not respond to warming through a simple physiological response, but rather to shifts in the structure and/or activity of the overall methane related microbial community. This more complex response to warming will affect how we predict changes in methane emissions under climate warming scenarios.

To rationalise both the disproportionate increases in CH₄ emissions and ratio of CH₄ to CO₂ after 11 years of warming, we measured the methane production capacity of the pond sediments at the same temperature (15°C) in the laboratory in controlled microcosms. Warmed pond sediments produced 2.5-fold more methane than their ambient controls (*post-hoc* pairwise comparisons: $p < 0.05$, Fig. 2a,b) for the same quality of carbon (carbon turnover k , t -statistic, $p = 0.053$, *see* also C to N ratio in Supplementary Table 2). The potential of sediments to produce methane increased equally in both the warmed and ambient ponds as carbon quality also increased (Fig 2b, $p = 0.4$). Warming has, however, stepped-up the fraction of carbon turned-over to methane because methanogens are now 1.5-fold more abundant in the warmed ponds (qPCR of the *mcrA* gene, Fig. 2c, circles, t -statistic, $p < 0.05$) and, importantly, methanogens in the long-term warmed ponds appeared to be ~60% more efficient at making methane too (Fig. 2c, triangles). This increase in methanogen efficiency explains the disproportionate increase in methane emissions (Fig. 1a) and, by increasing the ratio of CH₄ to CO₂ produced in the sediment by 3-fold (t -statistic, $p < 0.001$, Fig. 2d), also accounts for the increased ratio of CH₄ to CO₂ emitted to the atmosphere at night (Fig. 1b). These increases are, however, hard to rationalise without a fundamental change to the structure of the methanogen community.

In freshwater sediments, methane is produced predominantly by acetoclastic and hydrogenotrophic methanogenesis²⁴. Theoretically these two types of methanogenesis have stoichiometric equivalence and complete glucose degradation should produce CH₄ and CO₂ in a 1:1 ratio²⁵, with 33%

CH₄ from hydrogenotrophy and 67% CH₄ from acetoclastic methanogenesis (ref. 24, 25 and *see* Supplementary Discussion). Just as in our pond sediments (Fig. 2d), however, this idealised 1:1 ratio is seldom found with deviations from 1:1 being ascribed to differences in organic matter oxidation state, pH or organic matter quality^{27–29} that simply do not apply to our ponds. Alternatively, we would argue that the proportion of available H₂ flowing to methane increases under warming^{17,28} (*see* Supplementary Discussion) and that the increase in both methanogen efficiency and CH₄ to CO₂ ratios (Fig. 2c, 2d and 1b) suggested a shift towards hydrogenotrophic methanogenesis with long-term warming. We tested this hypothesis by analysing the methanogen communities and, in accordance, identified significant shifts in two dominant hydrogenotrophic genera between the warmed and ambient ponds (Fig. 3a and b and Supplementary Tables 3 and 4) but no significant changes in any other methanogens (e.g. acetoclastic genera). Specifically, the relative abundance of *Methanobacterium* increased significantly from 8.5% to 13.2% of the methanogen community, whereas, in contrast, *Methanospirillum* decreased from 31.3% to 22.7% between the ambient and warmed ponds, respectively (adjusted *p*-value <0.01, Fig. 3b). After 11 years of warming methanogen diversity was conserved (Supplementary Fig. 2) but marginal changes in the relative abundance of *Methanobacterium* and *Methanospirillum* and other minor changes within the community (with 4 hydrogenotrophic genera increasing in relative abundance and two new genera appearing in the warmed ponds; Supplementary Table 4) appeared to be linked to the increased contribution from hydrogenotrophic methanogenesis – increasing methane production and the ratio of CH₄ to CO₂ emitted. Other ecosystems, such as thawing peat permafrost, also show increased methane emissions on warming²³ but these are linked to fundamental successional changes in the methanogen community that match successional changes in the ecosystem. Yet, our freshwater ponds show that subtle shifts in the methanogen community can produce substantial changes to the methane emissions of these ecosystems under warming that would suggest natural freshwater systems are likely to be capable of responding in a similar manner (Fig 1c, ref. 7 and 28).

We performed further incubations with the addition of hydrogen and acetate (Fig. 3c) to identify a mechanism for these changes in the methanogen community and measured a disproportionate increase in methane production with hydrogen in the warmed pond sediments (Fig. 3c). Further short-term temperature manipulations also clearly showed that hydrogenotrophic methanogenesis was the most sensitive to temperature, with an apparent activation energy of 1.40 eV for H₂ compared to 0.7 eV for the controls (*post-hoc* pairwise comparisons: $p < 0.001$, Fig. 3d). Thus, warming makes hydrogenotrophic methanogenesis more favourable, providing a mechanism to drive the shift towards a more hydrogenotrophic methanogenesis due to warming.

Short-term (<3 months) experiments in wetlands have shown that the relative contribution of hydrogenotrophic methanogenesis decreases at lower temperatures^{17,28,30–32}. Conversely, hydrogenotrophy dominates in warmer freshwater environments and a community meta-analysis identified strong selection for hydrogenotrophic methanogens in warm environments^{33–35}. Here for the first time we demonstrate experimentally that long-term warming of a freshwater community favours hydrogenotrophic over acetoclastic methanogenesis, altering both the efficiency and structure of the methanogen community to increase the ratio of produced and emitted CH₄ to CO₂ (Fig. 3a, 3b, 2d and 1b). Our observations reflect subtle changes in the structural and functional ecology of shallow ponds in stark contrast to the major changes seen in hydrology, vegetation, organic matter quality and pH along a natural gradient of thawing permafrost²³, where increases in methane emissions run alongside major alteration to the methanogen community. Further, the predictable physiological increase in methane emissions seen after 1 year of experimental warming in peatland soils¹⁹, mirrors what we first observed in our ponds³⁶ - if ongoing warming sets peat on a similar trajectory, as our meta-analysis suggests, then we would predict disproportionate increases in methane emissions from peatlands too.

The balance between methane production and its oxidation controls the net emission of methane. We used similar laboratory microcosm incubations to those described above to investigate whether long-term warming enhanced methane oxidation to the same magnitude as methane production. In contrast to

methane production, however, we found the sediments' capacity to oxidise methane to be the same in both our warmed and ambient ponds (likelihood ratio test: $p=0.93$, Fig. 4a). The methanotrophs did have a strong kinetic potential to oxidise more methane and warming-induced increases in methane concentrations in the ponds (2.1-fold, Supplementary Table 2), were reflected in increased methane oxidation activity in the laboratory (1.9-fold, *see* equation (7) for Michaelis-Menten model). Similarly, while the temperature sensitivity of methane oxidation – in the laboratory – was the same in both warmed and ambient pond sediments (likelihood ratio test: $p=0.24$, Fig. 4b), the 4°C of warming *in situ* would increase methane oxidation activity too (i.e., 1.4-fold increase with the common activation energy of 0.57 eV in equation (2)). Altogether, higher methane concentrations and the 4°C of warming would increase the methane oxidation capacity of the warmed ponds by 2.6-fold (Supplementary Table 2). Further, as methanotrophic activity is confined to a thin, oxic zone at the sediment surface³⁷, which was ~40% shallower in the warmed ponds (Supplementary Fig. 3), there would have been an oxygen effect too. Combined, the methane kinetic, temperature and oxygen-penetration effects (1.9-, 1.4- and 1.4- fold, respectively) would drive 3.6-fold greater methane oxidation activity in the warmed ponds (*see* Supplementary Table 2 and further discussion there in) that ultimately attenuated ~95% of the extra methane production under warming but not the 98% required to prevent increased methane emissions. Which poses the question: why might methanotrophs not be able to keep-up with methanogens under warming?

Methanotroph abundance did increase in the warmed ponds but not enough (2.45-fold *v.s.* 2.67-fold required, *see* Supplementary Table 2) to offset the greater warming-induced methane production. As a proxy for their growth-efficiency¹⁶ we measured the fraction of methane assimilated into methanotroph biomass (carbon conversion efficiency i.e., CCE) in the laboratory. Accordingly, methanotroph CCE was indistinguishable between the warmed and ambient sediments, however, methanotroph CCE was suppressed at both higher methane concentrations and higher temperatures (Fig. 4c and d) i.e., the exact conditions induced by warming. In the ponds, therefore, the warmed methanotrophs would assimilate a

smaller fraction of their metabolised methane, grow less efficiently and thus lack the potential to reach the required abundance to balance greater methane production. Whereas we cannot predict the increase in methane production from a simple physiological response to warming, we could determine just such a simple physiological response for methane oxidation. In contrast to warming-induced change in the methanogen community, the methanotroph community was conserved (Supplementary Fig. 4 and Supplementary Table 3); it is noticeable, however, that 11 of the 16 detected OTUs had a lower relative abundance (with two genera being undetected) in the warmed ponds (Supplementary Table 5). We propose that whereas warming makes hydrogenotrophic methanogenesis more favourable, thus changing the methanogen community, there is no similar mechanism to favourably alter the methanotroph community.

Our long-term warming experiment provides a mechanistic understanding of a potential positive feedback warming loop in the freshwater methane cycle. In particular, warming increases the efficiency of methanogenesis and preferentially alters hydrogenotrophy while limiting the capacity of methanotrophs to consume methane by impaired growth, which, together, increase the global warming potential of the carbon gases emitted. These emergent properties increase methane emissions far beyond a simple physiological increase to warming alone and what we have witnessed under experimental warming is, in part, borne out at the global-scale as a disproportionate increase in the capacity of a variety of naturally warmer ecosystems (e.g. wetlands, croplands, forests and grasslands, *see* Methods) to emit more methane. Together, our findings strongly indicate that as Earth continues to warm, natural ecosystems will emit disproportionately more methane to the atmosphere in a positive feedback warming loop (Fig 5).

Acknowledgments

This study was supported by Queen Mary University of London and the U.K. Natural Environment Research Council (NE/M02086X/1, NE/M020886/1). We thank Ian Sanders and Felicity Shelley for technical and fieldwork assistance; James Pretty for mesocosm pond maintenance; Martin Rouen for

designing and installing the Campbell control and data-logging system; Hannah Prentice for collecting sediments and DNA extraction; Chloe Economou and Monika Struebig for help with molecular work; Patrick K.H. Lee for providing the *mcrA* database and related documents for bioinformatics analysis. We thank the principal investigators of the methane flux data products including William Quinton, Oliver Sonnentag, Georg Wohlfahrt, Sebastien Gogo, Ted Schuur, Ken Krauss, Ankur Desai, Gil Bohrer, Rodrigo Vargas, Dennis Baldocchi, Jiquan Chen, Housen Chu, Hiroki Iwata, Masahito Ueyama and Yoshinobu Harazono. We also thank the funding agencies that supported their flux measurements and the three anonymous reviewers whose comments greatly improved the manuscript.

Author contributions

M.T., Y.Z. and K.J.P conceived the study and Y.Z. conducted the vast majority of the experiments and analysed the data. Y.Z., M.T., K.J.P., G.Y.D. and A.J.D. discussed the data. Y.Z., M.T. and K.J.P. wrote the manuscript and all authors contributed to revisions. Y.Z. and S.H. set up the chamber system. Y.Z., O.E. and L.S. performed molecular analyses.

Competing interests

The authors declare no competing financial interests.

Additional Information

Supplementary information and **Extended Data Figures** are available in the online version of the paper.

Reprints and permissions information is available at www.nature.com/reprints.

Correspondence and requests for materials should be addressed to M.T. (m.trimmer@qmul.ac.uk).

222 References

- 223 1. Nisbet, E. G., Dlugokencky, E. J. & Bousquet, P. Methane on the Rise--Again. *Science* **343**, 493–
224 495 (2014).
- 225 2. Balcombe, P., Speirs, J. F., Brandon, N. P. & Hawkes, A. D. Methane emissions: choosing the
226 right climate metric and time horizon. *Environ. Sci. Process. Impacts* **20**, 1323–1339 (2018).
- 227 3. Holgerson, M. A. & Raymond, P. A. Large contribution to inland water CO₂ and CH₄ emissions
228 from very small ponds. *Nat. Geosci.* **9**, 222–226 (2016).
- 229 4. Saunio, M. *et al.* The global methane budget 2000–2012. *Earth Syst. Sci. Data* **8**, 697–751 (2016).
- 230 5. Bridgman, S. D., Cadillo-Quiroz, H., Keller, J. K. & Zhuang, Q. Methane emissions from
231 wetlands: Biogeochemical, microbial, and modeling perspectives from local to global scales. *Glob.*
232 *Chang. Biol.* **19**, 1325–1346 (2013).
- 233 6. Gudas, C. *et al.* Temperature-controlled organic carbon mineralization in lake sediments. *Nature*
234 **466**, 478–481 (2010).
- 235 7. Yvon-Durocher, G. *et al.* Methane fluxes show consistent temperature dependence across
236 microbial to ecosystem scales. *Nature* **507**, 488–91 (2014).
- 237 8. Allen, A. P., Gillooly, J. F. & Brown, J. H. Linking the global carbon cycle to individual
238 metabolism. *Funct. Ecol.* **19**, 202–213 (2005).
- 239 9. Hanson, R. S. & Hanson, T. E. Methanotrophic bacteria. *Microbiol. Rev.* **60**, 439–471 (1996).
- 240 10. Shelley, F., Abdullahi, F., Grey, J. & Trimmer, M. Microbial methane cycling in the bed of a chalk
241 river: oxidation has the potential to match methanogenesis enhanced by warming. *Freshw. Biol.* **60**,
242 150–160 (2015).
- 243 11. Mohanty, S. R., Bodelier, P. L. E. & Conrad, R. Effect of temperature on composition of the
244 methanotrophic community in rice field and forest soil. *FEMS Microbiol. Ecol.* **62**, 24–31 (2007).
- 245 12. Høj, L., Olsen, R. A. & Torsvik, V. L. Effects of temperature on the diversity and community
246 structure of known methanogenic groups and other archaea in high Arctic peat. *ISME J.* **2**, 37–48
247 (2008).
- 248 13. Hall, E. K. *et al.* Understanding how microbiomes influence the systems they inhabit. *Nat.*
249 *Microbiol.* **3**, 977–982 (2018).
- 250 14. Ho, A., Lüke, C. & Frenzel, P. Recovery of methanotrophs from disturbance: Population dynamics,
251 evenness and functioning. *ISME J.* **5**, 750–758 (2011).
- 252 15. Rocca, J. D. *et al.* Relationships between protein-encoding gene abundance and corresponding
253 process are commonly assumed yet rarely observed. *ISME J.* **9**, 1693–1699 (2015).
- 254 16. Trimmer, M. *et al.* Riverbed methanotrophy sustained by high carbon conversion efficiency. *ISME*
255 *J.* **9**, 2304–2314 (2015).
- 256 17. Fey, A. & Conrad, R. Effect of Temperature on Carbon and Electron Flow and on the Archaeal
257 Community in Methanogenic Rice Field Soil. *Appl. Environ. Microbiol.* **66**, 4790–4797 (2000).
- 258 18. Ho, A. & Frenzel, P. Heat stress and methane-oxidizing bacteria: Effects on activity and
259 population dynamics. *Soil Biol. Biochem.* **50**, 22–25 (2012).

- 260 19. Wilson, R. M. *et al.* Stability of peatland carbon to rising temperatures. *Nat. Commun.* **7**, 1–10
261 (2016).
- 262 20. Yvon-Durocher, G., Hulatt, C. J., Woodward, G. & Trimmer, M. Long-term warming amplifies
263 shifts in the carbon cycle of experimental ponds. *Nat. Clim. Chang.* **7**, 209–213 (2017).
- 264 21. Yvon-Durocher, G. *et al.* Five Years of Experimental Warming Increases the Biodiversity and
265 Productivity of Phytoplankton. *PLoS Biol.* **13**, 1–22 (2015).
- 266 22. Davidson, T. A. *et al.* Synergy between nutrients and warming enhances methane ebullition from
267 experimental lakes. *Nat. Clim. Chang.* **8**, 156–160 (2018).
- 268 23. McCalley, C. K. *et al.* Methane dynamics regulated by microbial community response to
269 permafrost thaw. *Nature* **514**, 478–481 (2014).
- 270 24. Conrad, R. Contribution of hydrogen to methane production and control of hydrogen
271 concentrations in methanogenic soils and sediments. *FEMS Microbiol. Ecol.* **28**, 193–202 (1999).
- 272 25. Wilson, R. M. *et al.* Hydrogenation of organic matter as a terminal electron sink sustains high
273 CO₂:CH₄ production ratios during anaerobic decomposition. *Org. Geochem.* **112**, 22–32 (2017).
- 274 26. Liu, Y. & Whitman, W. B. Metabolic, Phylogenetic, and Ecological Diversity of the
275 Methanogenic Archaea. *Ann. N. Y. Acad. Sci.* **1125**, 171–189 (2008).
- 276 27. Hodgkins, S. B. *et al.* Changes in peat chemistry associated with permafrost thaw increase
277 greenhouse gas production. *Proc. Natl. Acad. Sci. U. S. A.* **111**, 5819–5824 (2014).
- 278 28. Glissmann, K., Chin, K. J., Casper, P. & Conrad, R. Methanogenic pathway and archaeal
279 community structure in the sediment of eutrophic Lake Dagow: Effect of temperature. *Microb.*
280 *Ecol.* **48**, 389–399 (2004).
- 281 29. Inglett, K. S., Inglett, P. W., Reddy, K. R. & Osborne, T. Z. Temperature sensitivity of greenhouse
282 gas production in wetland soils of different vegetation. *Biogeochemistry* **108**, 77–90 (2012).
- 283 30. Conrad, R., Klose, M. & Noll, M. Functional and structural response of the methanogenic
284 microbial community in rice field soil to temperature change. *Environ. Microbiol.* **11**, 1844–1853
285 (2009).
- 286 31. Metje, M. & Frenzel, P. Methanogenesis and methanogenic pathways in a peat from subarctic
287 permafrost. *Environ. Microbiol.* **9**, 954–964 (2007).
- 288 32. Nozhevnikova, A. N. *et al.* Influence of temperature and high acetate concentrations on
289 methanogenesis in lake sediment slurries. *FEMS Microbiol. Ecol.* **62**, 336–344 (2007).
- 290 33. Wen, X. *et al.* Global biogeographic analysis of methanogenic archaea identifies community-
291 shaping environmental factors of natural environments. *Front. Microbiol.* **8**, 1–13 (2017).
- 292 34. Conrad, R. *et al.* Stable carbon isotope discrimination and microbiology of methane formation in
293 tropical anoxic lake sediments. *Biogeosciences* **8**, 795–814 (2011).
- 294 35. Kotsyurbenko, O. R. Trophic interactions in the methanogenic microbial community of low-
295 temperature terrestrial ecosystems. in *FEMS Microbiology Ecology* vol. 53 3–13 (2005).
- 296 36. Yvon-Durocher, G., Montoya, J. M., Woodward, G., Jones, J. I. & Trimmer, M. Warming
297 increases the proportion of primary production emitted as methane from freshwater mesocosms.
298 *Glob. Chang. Biol.* **17**, 1225–1234 (2011).

- 299 37. Reim, A., Lüke, C., Krause, S., Pratscher, J. & Frenzel, P. One millimetre makes the difference:
300 High-resolution analysis of methane-oxidizing bacteria and their specific activity at the oxic-
301 anoxic interface in a flooded paddy soil. *ISME J.* **6**, 2128–2139 (2012).
302

Figures

Fig. 1 | Ongoing divergence in methane emissions from the surface of our ponds mirrors natural warming. **a**, Emissions from our warmed and ambient ponds in 2007³⁶, 2013²⁰ and 2017 ($n=3553$, this study) have continued to diverge beyond that predicted for their 4°C difference in temperature (black-dashed line, equation 2, Methods). **b**, Ratio of CH₄ to CO₂ emitted at night ($n=4884$, *see* Methods) is 1.8-fold higher with warming (t -statistic, ***: $p<0.001$). **c**, Our disproportionate increase in methane emissions in 2017 (**a**), maps onto a trend of increasing capacity of naturally warmer ecosystems, including wetlands, croplands and forests (*see* Methods) to emit more methane - standardised to 15°C. Vertical and horizontal lines, 95% CI.

313 **Fig. 2 | Long-term warming increases methane production over methanogen abundance.** **a**, In the
314 laboratory ($n=238$, without additional substrates), warmed sediments produced more methane than
315 ambient sediments, standardised to 15°C. **b**, Production increased equally ($n=32$, $p=0.4$) with carbon
316 quality (k) in both treatments but warming stepped-up the fraction of carbon turned-over to methane
317 ($p<0.01$). **c**, Warming increased methanogen abundance (circles) and methanogen efficiency (activity,
318 triangles, $n=79$). **d**, Ratio of CH₄ to CO₂ produced by warmed sediments was ~3-fold higher than ambient
319 sediments ($n=218$). As ~95% of CH₄ is oxidised to CO₂ before emission from the ponds, the laboratory
320 CH₄ to CO₂ ratio is higher (Fig. 1b). Vertical lines, 95% CI. * $p<0.05$; ** $p<0.01$; *** $p<0.001$.

Fig. 3 | Long-term warming provides a mechanism to selectively alter the methanogen community.

a, Significant shifts in the methanogen community between ambient and warmed ponds ($n=79$, principal coordinate analysis at genus level, *see* Methods) were due to **b**, significant shifts in the relative abundance of two hydrogenotrophic genera (*Methanospirillum* and *Methanobacterium*). **c**, Hydrogen stimulated methanogenesis in the warmed pond sediments above that for acetate ($n=662$, vertical lines, 95% CI, statistical significance compared to the controls ~~***~~ and between the warmed and ambient ponds by * between the means (* $p<0.05$, ** $p<0.01$, *** $p<0.001$)). **d**, Hydrogenotrophy is more sensitive to temperature and warming makes hydrogenotrophy more favourable, selectively altering the methanogen community.

Fig. 4 | Methane oxidation is conserved and the growth of methanotrophy impaired under warming.

a, Strong physiological response in methane oxidation to higher methane in the laboratory, with a comparable capacity in warmed and ambient pond sediments ($n=158$, $p>0.05$ for V_{max} and k_m) and **b**, a similarly conserved response to temperature ($n=192$, $p=0.068$). Methanotrophic growth efficiency (i.e., carbon conversion efficiency, CCE %) was impaired at **c**, higher methane concentrations ($n=69$, $p<0.01$) and **d**, higher-temperatures ($n=191$, $p<0.01$) i.e., the conditions induced by warming in the ponds. Under substrate limitation and impaired growth, the methanotroph community was conserved and lacked the potential to reach the required abundance to balance the increase in methane production under warming.

Fig. 5 | Positive climate warming feedback loop revealed by our long-term experiment. Methane emissions cannot be predicted by temperature alone and both the magnitude of emission and the ratio CH₄ to CO₂ increase as apparent emergent properties of changes in the overall methane cycle (red arrow). Long-term warming favours hydrogenotrophic methanogenesis, providing a mechanism to alter both the efficiency (yellow rectangle) and structure of the methanogen community (green rectangle). In contrast, there is no similar mechanism to alter the methanotroph community and physiological responses dominate. Methane oxidation cannot offset the extra methane production under warming (blue rectangle), and a positive feedback loop in the methane cycle develops through global warming.

Extended Data Figures

Extended Data Fig. 1 | Schematic of experimental pond set-up and dynamic chamber

measurements. Twenty artificial ponds, with 10 warmed (red) by 4°C above 10 ambient (blue) ponds, were paired in a randomized block design **(a)** and controlled via two temperature sensors (T1, T2), a thermocouple (T-stat) and a solid-state relay (SSR) **(b)**. Dynamic LI-COR chambers, floating on lifebuoys, were installed on 7 each of the warmed and ambient ponds **(c)**. Each floating chamber was connected to one of the inlet ports on the MIU and the MIU outlet port was connected to the gas inlet port of Ultra-Portable Greenhouse Gas Analyzer (LGR) **(d)**. A dynamic chamber is sequentially triggered to close by customised Campbell control unit (CCU) for 30 minutes for gas measurements while the other chambers remain open. When a chamber is triggered to close, the MIU switches simultaneously to the inlet connected to the closing chamber to direct its gas flow to the LGR. *See Methods and Extended Data Fig. 2 for further details on methane emissions.*

Extended Data Fig. 2 | Consistent seasonal patterns in daily methane emissions under warming but with ongoing divergence over 10 years (2007³⁶, 2013²⁰ and 2017 (this study)). The seasonal patterns in all 3 years are very similar, despite the use of different techniques but the frequent measurements (three times daily) using dynamic chambers in 2017 captured far more details in emissions compared to 2007 and 2013 when static chambers were used to measure methane emission on 7 and 12 occasions over each year, respectively. Note the natural log scale for methane emissions.

368 **Extended Data Fig. 3 | Methane emissions at night and during the day.** Methane emissions during the
369 day (**a**) and at night (**b**) follow the similar seasonal patterns; yet the methane emissions at night are
370 significantly greater than during the day (**c**).

371

Methods

Mesocosm pond facility

Twenty artificial ponds were installed in 2005 at the Freshwater Biological Association's River Laboratory in Dorset, UK (2°10'W, 50°30'N). The ponds (1.8m diameter and 2.5m²) hold 1m³ of water (50cm deep), have a 6-10cm layer of fine sand sediment and were seeded with local communities of macroinvertebrates and plants to mimic shallow lakes^{20,21,36}. The ponds are arranged in a randomised-block design, with half of the ponds being warmed by 4°C above ambient temperatures since 2006 (Extended Data Figure 1).

Methane and carbon dioxide emissions from the surface of the ponds

Methane and carbon dioxide emissions from the surface of the ponds were measured ~3 times per day from February 2017 to February 2018 using a combination of an Ultra-Portable Greenhouse Gas Analyzer (915-0011, LGR, Los Gatos Research), a Multi-port Inlet Unit (MIU, LGR), 14 dynamic chambers (Ø 20cm, 0.43L, 8100-101, LI-COR) and a customised Campbell control unit (CCU) (Extended Data Figure 1). Each dynamic chamber floats on a ring permanently fixed at the centre of 7 of the 10 warmed and 7 of the 10 ambient ponds and are connected to 1 to 14 of the inlet ports on the MIU which is connected to the inlet port of the LGR that pumps air at ~3 L min⁻¹. As the LGR cannot operate the dynamic chambers directly, the CCU triggers them sequentially after receiving a signal from the LGR. Each chamber remains open until triggered to close for a 30-minute sampling period, at which point the MIU switches to the closing chamber to direct gas to the LGR. A complete cycle takes ~8h, including background atmospheric methane. Between each chamber the CCU synchronizes the MIU and LGR to avoid any drift in the sequence. Data were acquired at 1Hz and methane or carbon dioxide emissions calculated at steady-state by³⁸:

$$F = \frac{(C_{\text{observation}} - C_{\text{background}})}{S_{\text{area}}} \times \frac{V_{\text{aeration}}}{dt} \quad (1)$$

Where F is the emission ($\mu\text{mol m}^{-2} \text{h}^{-1}$), $C_{\text{observation}}$ is the concentration of methane or carbon dioxide ($\mu\text{mol L}^{-1}$) at steady-state (estimated by averaging the concentrations) and $C_{\text{background}}$ their respective atmospheric concentrations ($\mu\text{mol L}^{-1}$), V_{aeration}/dt is the volume of air flowing through a chamber per hour and S_{area} is the surface area of the chamber (0.031 m^2). We also needed to characterise ebullition events that lead to rapid increases in methane concentrations over short periods of time and bias our emission estimates (see Supplementary Fig. 6 for examples). Ebullition events were identified as a consistent increase in methane concentrations over 5 seconds at a rate greater than 50ppb per second, to a maximum concentration, or consistent decrease for 5 seconds, at a rate greater than 10ppb per second, after the post-ebullition maxima. We acknowledge that these criteria also identify other non-steady flux events besides ebullition and we subsequently distinguished these events from ebullition if their maximum methane concentration was lower than atmospheric methane i.e., noise. Of the 16504 total chamber measurements, 198, i.e., 1.2%, were identified as ebullition and 7, i.e., 0.04%, were identified as other non-steady-state events. Both ebullition and other non-steady flux events were excluded from further calculations.

Predicting methane emissions, production and oxidation from their apparent activation energies

Activation energy is a measure of temperature sensitivity^{7,8}. For example, the common activation energy for methane emission of 0.96 eV, predicts a 1.70-fold increase in emissions under our 4°C warming scenario according to:

$$\frac{R(T_W)}{R(T_A)} = e^{\frac{E_a}{kT_W} - \frac{E_a}{kT_A}} \quad (2)$$

Where $R(T)$ is the metabolic rate (e.g. methane emission and similarly for production or oxidation) and T_W and T_A are the mean annual temperatures of the warmed and ambient ponds (288.15 and 292.15K, respectively). k is the Boltzmann constant ($8.62 \times 10^{-6} \text{ eV K}^{-1}$).

Potential methane production with temperature and additional substrates

The pond setup provided 10 independent replicates for the warmed and ambient pond treatments (Extended Data Figure 1). Three cores of intact sediment (typically 6cm to 10cm depth) were collected by hand using small Perspex corers (\varnothing 34mm \times 300mm) and butyl stoppers, every month from January, 2016, to December, 2016, (except for July) from three to five warmed and ambient ponds (4 on average), selected randomly. Intact cores of sediment were stored in zip-lock bags and kept cool with freezer blocks for transport back to laboratory (<4h) and then kept in the dark at 4°C.

Sub-samples (~3g) of the bottom sediment layers (below 4cm) from the same pond were homogenised, thus no further pseudo-replication was included within each pond, and aliquoted into gas-tight vials (12ml, Labco, Exetainer®) inside an anoxic glove box (CV204; Belle Technologies) filled with oxygen-free nitrogen (OFN, BOC). The capacity and temperature sensitivity of methanogenic potentials with either additional acetate or hydrogen as substrates were quantified. For acetate, pond water (3.6ml) and acetate stock solutions (0.4ml, 100mM, Sigma-Aldrich®, for molecular biology) were flushed with OFN for 10 minutes and then added to each vial to create final concentrations of 10mM and the vials sealed. For hydrogen, 4ml OFN-flushed pond water were added to each vial, the vials sealed and injected with 1ml of the pure hydrogen (H₂, research grade, BOC, Industrial Gases, Guilford, UK) to create an ~17% H₂ headspace (v/v). A further set of vials were left unamended as controls (see Supplementary Table 7 for sample size). All the prepared vials were then incubated in separate batches at approximately 12°C, 17°C, 22°C and 26°C (precise temperature could vary by 2°C between months) for up to 4 days and shaken by hand twice per day. The production of methane and carbon dioxide was quantified every 24h using a gas chromatogram fitted with a hot-nickel methanizer and flame-ionization detector (Agilent Technology UK Ltd., South Queensferry, UK), as before^{16,39}.

Methane oxidation and its carbon conversion efficiency

Three sediment cores were collected from 8 warmed and 8 ambient ponds using truncated syringes (25ml) in May, June and July, 2017, to measure the temperature sensitivity and capacity of methane oxidation. In

December, 2018, three sediment cores were collected from the same ponds to measure the kinetic concentration effect on methane oxidation rates. The sediment cores were kept cool and transported as described above.

The top 2cm of sediment from each pond was homogenised and transferred into gas-tight vials (12ml, Labco, Exetainer®) along with the overlying pond water (4ml). The vials then sealed to leave a headspace of air. We quantified the effect of long-term warming on both the temperature and kinetic response of methane oxidation. For temperature, we enriched the vials with 200µL of ¹³C-CH₄ (99% atom) to 40µmol L⁻¹ in the water phase. Control vials were set up without ¹³C-CH₄ enrichment and all vials incubated with gentle shaking (130 rpm) at 5°C, 10°C, 15°C and 22°C to mix the ¹³C-CH₄ throughout the slurry. Methane concentrations described here are higher than in our ponds to enable short incubations (~22h) at the different temperatures and avoid being confounded by substrate limitation (*see* kinetics). For the kinetic response, the vials were enriched with ¹³C-CH₄ to 1 to 60 µmol L⁻¹ in the water phase and the vials incubated as above at 22°C. Vials below 15µmol L⁻¹ ¹³C-CH₄ were incubated for <12h and those higher initial incubated for ~20h when the experiments were fixed by injecting 200µL ZnCl₂ (50% w/v).

The carbon conversion efficiency of methanotrophy was estimated using the fraction of ¹³C-CH₄ recovered as ¹³C-inorganic carbon as per¹⁶: $1 - \frac{\Delta^{13}\text{C-inorganic}}{\Delta^{13}\text{C-CH}_4}$ where Δ represents the production of ¹³C-inorganic or the consumption of ¹³C-CH₄.

Oxygen profile measurements

Dissolved oxygen concentrations in the water overlying the sediments were measured from October, 2015, to October, 2016, in 7 warmed and 7 ambient ponds, using oxygen sensors (miniDOT oxygen logger, PME, California USA) at 10 minute intervals. Penetration of oxygen into the sediments was measured in April, 2016, at a resolution of 100µm, as described in⁴⁰.

Statistical analysis

All statistical analyses were performed in R (3.2.5)⁴¹.

Annual methane emissions

Rates of methane emission were natural log-transformed and fitted into Generalized additive mixed effect models (GAMMs) to characterize the average annual emission patterns for the warmed or ambient ponds as a fixed effect, as before²⁰. The annual rates of methane emissions were calculated using the parameter estimates from the best GAMMs model (Supplementary Table 6) and extrapolated to a year by multiplying by 365.

Ratio of CH₄ to CO₂ emitted from the surface of the ponds and produced in anoxic sediments

Our artificial ponds are net sinks for CO₂^{20,21}. To illustrate the connection between our sediment potential measurements for CH₄ and CO₂ production in the laboratory, we compared them to the emission ratio for CH₄ and CO₂ from the ponds at night when they emitted both CH₄ and CO₂. Before statistical analysis, the ratio data above the 95th percentiles for each treatment were characterized as outliers and removed. The significance of the main treatment effect i.e., warmed or ambient ponds, was then determined using the *t*-statistic.

Meta-analysis on methane emission capacity across a natural temperature gradient

There were 491 datasets available on the AmeriFlux (<http://ameriflux.lbl.gov/>) and EuroFlux network (<http://www.europe-fluxdata.eu/>) (Supplementary Table 1). Of those, only 26 were for methane and air-temperature and only 19 of the available sites covered at least 6 months of the year and demonstrated a good relationship ($p < 0.05$) between methane emission and air-temperature. Half-hour aggregated eddy-covariance data were downloaded for these 19 sites which are wetlands (68%), forests, grasslands and shrubs (21%) and croplands (11%). The original methane emissions rates ($\text{nmol CH}_4 \text{ m}^{-2} \text{ s}^{-1}$) were then integrated to give daily estimates of methane emissions ($\mu\text{mol CH}_4 \text{ m}^{-2} \text{ d}^{-1}$).

Daily rates of methane emission were then standardized to 15°C to provide comparable estimates of methane emission capacities between sites using the Boltzmann-Arrhenius relationship:

$$\ln ME_i(T) = E_{ME} \left(\frac{1}{kT_{15}} - \frac{1}{kT_i} \right) + \ln ME(T_{15}) \quad (3)$$

Where $\ln ME_i(T)$ is the natural-logarithm-transformed rate of daily methane emissions by any site i ($i = 1, 2, \dots, 19$) under air-temperature T in Kelvin. k is the Boltzmann constant and $\left(\frac{1}{kT_{15}} - \frac{1}{kT_i} \right)$ is standardized temperature for site i . T_{15} (15°C equals 288.15K) is the temperature used to center the temperature data. Therefore, the slope term E_{ME} represents the temperature sensitivity and the intercept $\ln ME(T_{15})$ is the estimated daily “capacity” of methane emission standardized to 15°C. The standardized methane emission capacities $\ln ME(T_{15})$ were then modelled as a simple linear function of annual average site temperatures using the “lm” function.

Temperature sensitivity and capacity of methane production and oxidation

We estimated the temperature sensitivity and capacity of methane production and oxidation using the Boltzmann-Arrhenius equation⁷:

$$\ln F_{ij}(T) = (\bar{E} + a_i + a_j) \left(\frac{1}{kT_C} - \frac{1}{kT_{ij}} \right) + (\overline{\ln F(T_C)} + b_i + b_j) \quad (4)$$

Where $F_{ij}(T)$ is the rate of methane production or oxidation by sediment from pond i ($i=1, 2, \dots$), collected in month j ($j=1, 2, \dots$). As our experimental design yielded replicate responses in ponds for both treatments over months, we treated sampling month and replicate pond as crossed random effects on the slope ($a_i + a_j$) and the intercept ($b_i + b_j$) of the models to account for the random variation among months and ponds from the fixed effect. Methane oxidation experiments were performed in only three months, therefore the parameter “sampling month” was not included to improve model convergence. The slope \bar{E} of equation (4) represents the estimated population activation energy (temperature sensitivity) in units of eV, for either methane production ($\overline{E_{MP}}$) or oxidation ($\overline{E_{MO}}$). k is the Boltzmann constant. We standardized the plot using the term $\frac{1}{kT_C}$, in which T_C (288.15K) is the average temperature in the ambient ponds *i.e.*, 15°C in 2017, so that the terms, $\overline{\ln F(T_C)}$ corresponds to the average capacity of methane

production or oxidation at T_C . The effect of treatment (i.e., ambient or warmed ponds) and substrates on methane production, on both the slope (temperature sensitivity) and intercept (average capacity of methane production or oxidation at T_C) were modelled as fixed effects.

The data were fitted into linear mixed-effect models (LMEM) using the lme4 package⁴². The details of model fitting, selection and validation are provided in Supplementary Table 7 and 9 for production and oxidation, respectively. After the best fitting model was determined, *post-hoc* pairwise comparisons of the estimated marginal means of methane production capacity and temperature sensitivity were obtained using the “emmeans” package⁴³.

Turnover decay constants for organic carbon

We derived turnover decay constants k (h^{-1}) as a relative indicator of sediment carbon quality⁴⁴:

$$k = \frac{R}{C} \quad (5)$$

Where R is the rate of CO_2 production standardized to 15°C ($\text{nmol g}^{-1} \text{h}^{-1}$) in anoxic slurry incubations and C the concentration of organic carbon (nmol g^{-1}). To characterize the proportion of organic carbon converted to methane in the sediments, we fitted k as an explanatory variable into a mixed effect model:

$$\ln MG_j = (\text{slope} + a_j) \times \ln k + (\text{intercept} + b_j) \quad (6)$$

Where $\ln MG_j$ is the natural logarithm of methane production capacity standardized to 15°C by any sediment collected in month j ($j=1, 2, \dots$) and $\ln k$ is the natural logarithm of k . The slope represents the potential to produce methane in response to carbon quality and the intercept the proportion of organic carbon converted to methane, i.e., methane produced per unit carbon turned over. The random effect terms a_j and b_j represent variation among sampling months. The effect of treatment (i.e., warmed or ambient) on the intercept and slope were fitted into the model as a fixed effect and its significance tested using the Likelihood Ratio Test (LRT) (Supplementary Table 8).

Kinetic concentration effect on rates of methane oxidation

The kinetic concentration effect on rates of CH₄ oxidation was characterised using a Michaelis-Menten model:

$$MO_i(C_{CH_4}) = \frac{(V_{max} + a_i) \times C_{CH_4}}{(K_M + b_i) + C_{CH_4}} \quad (7)$$

Where MO_i is the rate of ¹³C-CH₄ oxidation by any sediment of pond i ($i=1, 2, \dots$). C_{CH_4} is the initial ¹³C-CH₄ concentration. The parameters V_{max} and K_M were determined by fitting self-starting nonlinear mixed-effect models. The mesocosm ponds were fitted into the models as random effects to account for their variations on the parameter V_{max} (a_i) and on the parameter K_m (b_i) and the significance of warmed or ambient ponds tested using LRT (Supplementary Table 9).

Carbon conversion efficiency of methanotrophy

To characterise temperature and kinetic effects on the carbon conversion efficiency (CCE), we fitted CCE as a response variable into a mixed effect model:

$$CCE_i(T) = (slope + a_i) \times (T - T_C) + (\overline{CCE(T_C)} + b_i) \quad (8)$$

$$CCE_i(C_{CH_4}) = (slope + a_i) \times C_{CH_4} + (\overline{CCE(C_{CH_4,0})} + b_i) \quad (9)$$

Where $CCE_i(T)$ and $CCE_i(C_{CH_4})$ are the CCE (%) by any sediment from pond i ($i=1, 2, \dots$) at temperature T or with an initial concentration of ¹³C-CH₄ C_{CH_4} . To quantify the temperature sensitivity, again, we centered the plot to the average annual temperature in the ambient ponds (15°C), so that the term $\overline{CCE(T_C)}$ represents the average CCE at 15°C. However, we did not center equation (9) and the intercept term $\overline{CCE_i(C_{CH_4,0})}$ is the CCE estimate at 0 μmol L⁻¹. The random effect terms a_i and b_i represent variation among ponds and the effect warmed or ambient ponds on the intercept and slope were fitted and tested as above (Supplementary Table 10).

Microbial community analysis

Sediment sampling and DNA extraction

Monthly sediment samples were collected from March 2016 to August 2017 from 8 warmed and 8 ambient ponds using cut-off 25mL syringes. The top 2cm of sediment was transferred into an Eppendorf tube and the rest into a Falcon tube and stored at -80°C. DNA was extracted from 0.5g of wet sediment (DNeasy[®] PowerSoil[®] Kit; Qiagen) and DNA yield quantified using NanoDrop (Thermo Scientific) according to manufacturer's instructions; yield was 1-4 µg g⁻¹ wet sediment.

PCR amplification and sequencing

The *mcrA* gene, a methanogen molecular marker, was amplified using *mcrIRD* primers⁴⁵ (forward: 5'-TWYGACCARATMTGGYT-3'; reverse: 5'-ACRTTCATBGCTARTT-3'). PCRs were performed in 50µL containing 25µL of MyTaq[™] Red Mix (Bioline), 1µL of each primer (10µM), 3µL of DNA template and 20µL of molecular biology quality water. Amplifications were performed in a T100[™] Cyclor (Bio-Rad) following the thermal program: (1) 95°C for 5 min, (2) 40 cycles at 95°C for 45s, 51°C for 45s and 72°C for 60s, (3) 72°C for 5min.

The *pmoA* gene, a methanotroph molecular marker, was amplified using a semi-nested PCR with A189F (5'-3': GGNGACTGGGACTTCTGG) - A682R(5'-3': GAASGCNGAGAAGAASGC) in the first round and A189F (5'-3': GGNGACTGGGACTTCTGG) - A650R (5'-3': ACGTCCTTACCGAAGGT) in the second round⁴⁶. PCRs were performed in 25 µL containing: 12.5µL of MyTaq[™] Red Mix (Bioline), 1µL of each primer (10µM), 1µL of DNA and 9.5µL of molecular biology quality water. For the first round, a touch-down PCR⁴⁶ was performed in a T100[™] Cyclor (Bio-Rad) following the thermal program: (1) 94°C, 3 min, (2) 30 cycles at 94°C, 45 s, 62 to 52°C, 60 s (initially decreasing by 0.5°C per cycle down to 52°C) and 72°C, 180s, (3) 72 °C, 10 min. The second round followed the thermal program: (1) 94 °C, 3 min, (2) 22 cycles at 94 °C, 45 s, 56 °C, 60 s and 72 °C, 60 s, (3) 72 °C, 10 min. PCR products were checked by agarose gel electrophoresis and stained with GelRed[®].

Before sequencing, PCR products were cleaned using Agencourt[®] AMPure[®] XP beads (Beckman Coulter). Barcodes and linkers were added by a 10-cycle PCR (95°C, 3 min, 10 cycles of 98°C, 20s, 55°C, 15s and 72°C, 15s, 72°C, 5min). Final PCR products were quantified with a Qubit 2.0 Fluorometer (Invitrogen). 250 ng of PCR product from each sample was normalised to 4 nmoles (SequalPrep Normalization Plate Kit, Invitrogen) and combined for sequencing on the Illumina MiSeq platform (300 bp paired-end) at the Genomics Service, University of Warwick (UK).

Processing of sequence data

Downstream sequence analysis was conducted using QIIME2 (2018.2.0)⁴⁷ on the Apocrita HPC facility at Queen Mary University of London, supported by QMUL Research-IT⁴⁸. Paired-end de-multiplexed files were imported into QIIME2 and processed using DADA2 for modelling and correcting amplicon errors⁴⁹. Primer sequences were trimmed, low-quality sequences (QS <35) and chimeras were removed. Amplicon Sequence Variants (ASVs) were then inferred by DADA2. To analyse the data at genus-level, ASVs were clustered first into species-level Operational Taxonomic Units (OTUs) at 85% similarity for *mcrA* and 90% for *pmoA* sequences^{50,51}. OTUs were named using the pre-trained Naïve Bayes classifier using custom databases^{52,53} to specific genus-level clusters (Supplementary Table 4 and 5). The classifier was trained on sequences extracted for the appropriate *mcrA* and *pmoA* gene fragments.

One *mcrA* sample was not analysed as it contained too few sequence reads. The final dataset contained 68 unique *mcrA* OTUs from 1,633,993 reads and 65 unique *pmoA* OTUs from 2,013,666 reads.

Phylogenetic analysis

Classified sequence data was further analysed using “phyloseq” in R⁵⁴.

Variation in richness (α -diversity)

For each sample, OTU richness, Chao1 index, Shannon’s diversity index and evenness were calculated.

The differences between treatments were determined using mixed effect models, fitting each experimental

pond as a random effect. To test the significance of long-term warming on α -diversity LRT was performed comparing full and reduced models (Supplementary Fig. 2 and 5).

Variation in community composition (β -diversity)

Principal Coordinate Analysis (PCoA) was used to analyse the communities between treatments using a Bray-Curtis dissimilarity index with Hellinger standardized datasets at genus level. The scores of the samples along the PCoA axes, with the two largest eigenvalues, were fitted into mixed-effect model and the significance of long-term warming on scores was tested as above⁴² (Supplementary Table 3). PERMANOVA⁵⁵ with the “adonis” function (vegan package)⁵⁶ was used to partition variation in a distance matrix between treatments using a permutation test with pseudo-*F* ratios with similar results to the PCoA.

Differences in taxonomic abundance

Changes in abundance under warming was investigated using a negative binomial generalized linear model using DESeq2⁵⁷. DESeq2 was designed for RNA-seq data but has been used to analyse microbiome data⁵⁷ especially if libraries are evenly sized. Change under warming at genus level was estimated by setting the false discovery rate to 0.01.

Quantitative PCR (qPCR) of methanogens and methanotrophs.

Methanogen and methanotroph population sizes in sediment DNA samples was determined using qPCR with the mcrIRD primers (*mcrA*) and A189F-A650 primers (*pmoA*), respectively. Amplifications were performed using CFX384 TouchTM Real-Time PCR (Bio-Rad) in a total volume of 10 μ L containing: 5 μ L of SsoAdvancedTM Universal SYBR[®] Green Supermix (Bio-Rad), 0.2 μ L of each primer (10 μ M), 1 μ L of DNA template and 3.6 μ L of molecular biology quality water. Standard curves (10²-10⁷ copies μ L⁻¹) were constructed by serial diluting plasmid DNA containing *mcrA* or *pmoA* gene inserts.

The qPCR program for *mcrA* was: (1) 98°C, 3min; (2) 40 cycles at 98°C, 15s, 55°C, 15s and 72°C, 60s; (3) 95°C, 10s and for *pmoA* was: (1) 96°C, 5min; (2) 40 cycles at 94°C, 45s, 60°C, 45s and at 72°C, 45s. Products specificity and size were confirmed by melt curve analysis after the final extension.

Cell-specific activities of methanogens and methanotrophs

Cell-specific activities were calculated for both methanogens and methanotrophs by dividing CH₄ production and oxidation capacity at 15°C by *mcrA* and *pmoA* gene copy abundances respectively.

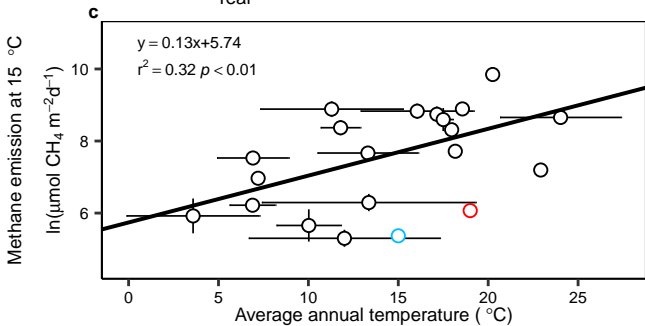
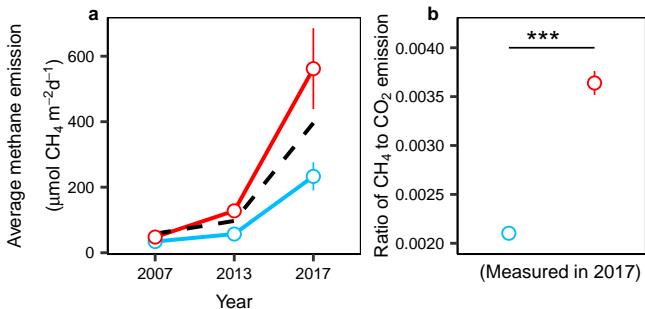
Data availability.

The data that support the findings of this study are available from the corresponding author upon request. DNA sequences are in the National Center for Biotechnology Information database, under BioProject ID PRJNA484117.

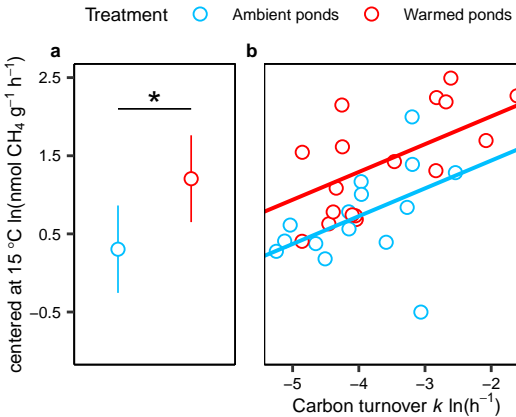
38. Yver Kwok, C. E. *et al.* Methane emission estimates using chamber and tracer release experiments for a municipal waste water treatment plant. *Atmos. Meas. Tech.* **8**, 2853–2867 (2015).
39. Sanders, I. A. *et al.* Emission of methane from chalk streams has potential implications for agricultural practices. *Freshw. Biol.* **52**, 1176–1186 (2007).
40. Neubacher, E. C., Parker, R. E. & Trimmer, M. Short-term hypoxia alters the balance of the nitrogen cycle in coastal sediments. *Limnol. Oceanogr.* **56**, 651–665 (2011).
41. R Core Team. R: A Language and Environment for Statistical Computing. (2014).
42. Kuznetsova, A., Brockhoff, P. B. & Christensen, R. H. B. {lmerTest} Package: Tests in Linear Mixed Effects Models. *J. Stat. Softw.* **82**, 1–26 (2017).
43. Lenth, R. emmeans: Estimated Marginal Means, aka Least-Squares Means. (2019).
44. Nicholls, J. C. & Trimmer, M. Widespread occurrence of the anammox reaction in estuarine sediments. *Aquat. Microb. Ecol.* **55**, 105–113 (2009).
45. Lever, M. A. & Teske, A. P. Diversity of methane-cycling archaea in hydrothermal sediment investigated by general and group-specific PCR primers. *Appl. Environ. Microbiol.* **81**, 1426–1441 (2015).
46. Horz, H. P., Rich, V., Avrahami, S. & Bohannan, B. J. M. Methane-oxidizing bacteria in a

- California upland grassland soil: Diversity and response to simulated global change. *Appl. Environ. Microbiol.* **71**, 2642–2652 (2005).
47. Caporaso, J. G. *et al.* QIIME allows analysis of high-throughput community sequencing data. *Nat. Methods* **7**, 335–336 (2010).
 48. King, T., Butcher, S. & Zalewski, L. Apocrita - High Performance Computing Cluster for Queen Mary University of London. (2017) doi:10.5281/ZENODO.438045.
 49. Callahan, B. J. *et al.* DADA2: High-resolution sample inference from Illumina amplicon data. *Nat. Methods* **13**, 581–583 (2016).
 50. Pester, M., Friedrich, M. W., Schink, B. & Brune, A. *pmoA*-based analysis of methanotrophs in a littoral lake sediment reveals a diverse and stable community in a dynamic environment. *Appl. Environ. Microbiol.* **70**, 3138–3142 (2004).
 51. Oakley, B. B., Carbonero, F., Dowd, S. E., Hawkins, R. J. & Purdy, K. J. Contrasting patterns of niche partitioning between two anaerobic terminal oxidizers of organic matter. *ISME J.* **6**, 905–914 (2012).
 52. Wilkins, D., Lu, X. Y., Shen, Z., Chen, J. & Lee, P. K. H. Pyrosequencing of *mcrA* and archaeal 16S rRNA genes reveals diversity and substrate preferences of methanogen communities in anaerobic digesters. *Appl. Environ. Microbiol.* **81**, 604–613 (2015).
 53. Yang, Sizhong; Wen, Xi; Liebner, S. *pmoA* gene reference database (fasta-formatted sequences and taxonomy). *GFZ Data Services* (2016).
 54. McMurdie, P. J. & Holmes, S. phyloseq: An R Package for Reproducible Interactive Analysis and Graphics of Microbiome Census Data. *PLoS One* **8**, e61217 (2013).
 55. Anderson, M. J. Permutational Multivariate Analysis of Variance (PERMANOVA). in *Wiley StatsRef: Statistics Reference Online* 1–15 (Wiley, 2017).
 56. Oksanen, J. *et al.* vegan: Community Ecology Package. (2018).
 57. Love, M. I., Huber, W. & Anders, S. Moderated estimation of fold change and dispersion for RNA-seq data with DESeq2. *Genome Biol.* **15**, 550 (2014).

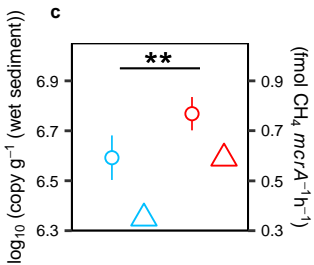
Treatment ○ Ambient ponds ○ Warmed ponds ○ Natural ecosystems



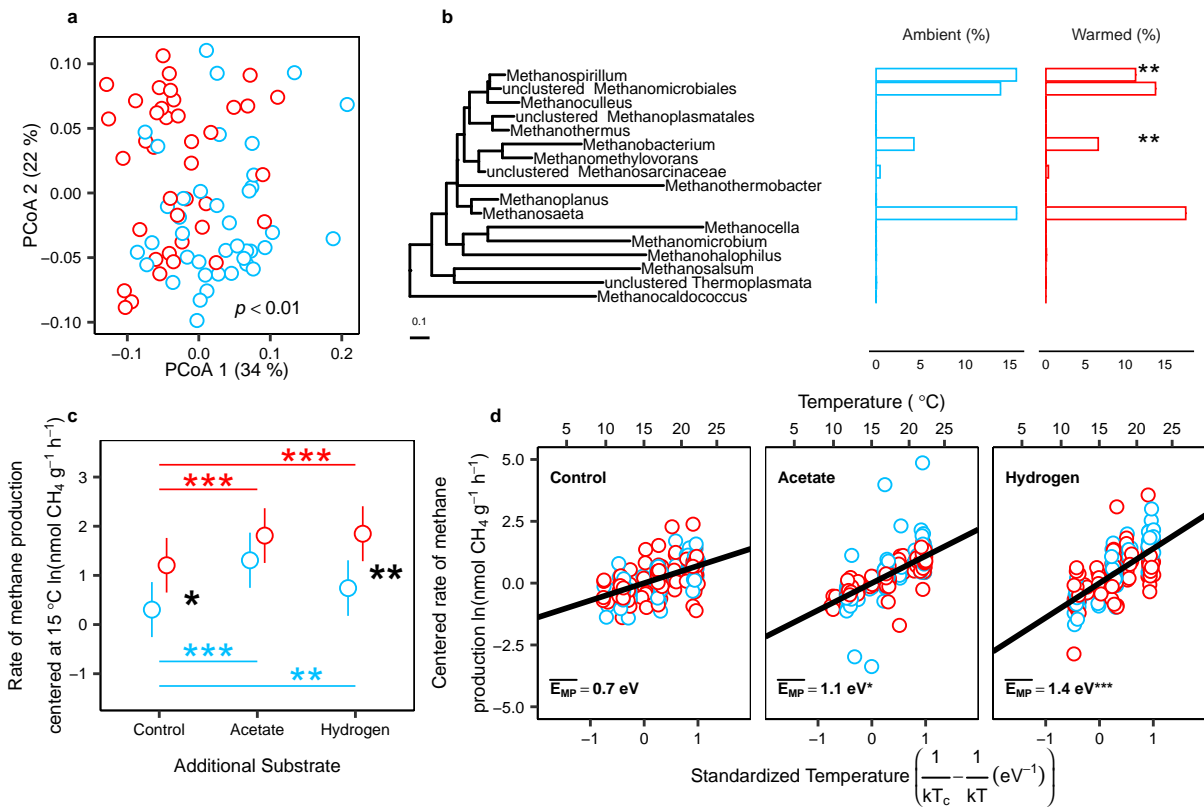
Rate of methane production



mcrA abundance

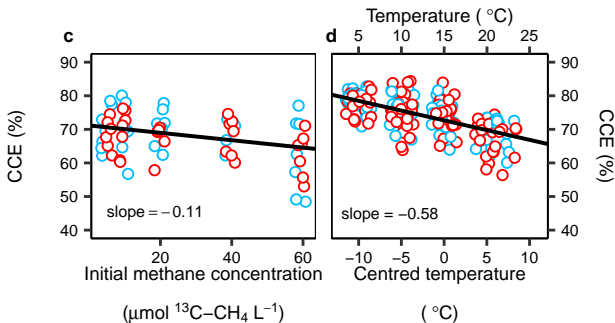
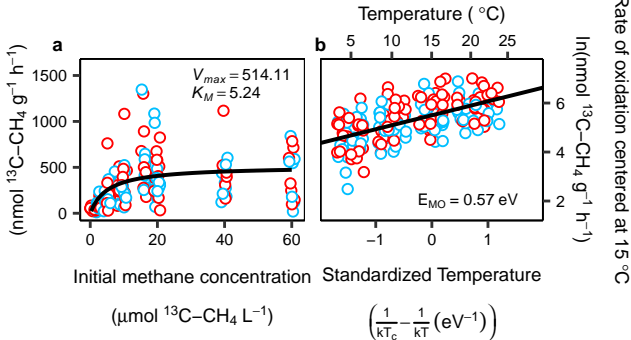


Treatment ○ Ambient ponds ○ Warmed ponds

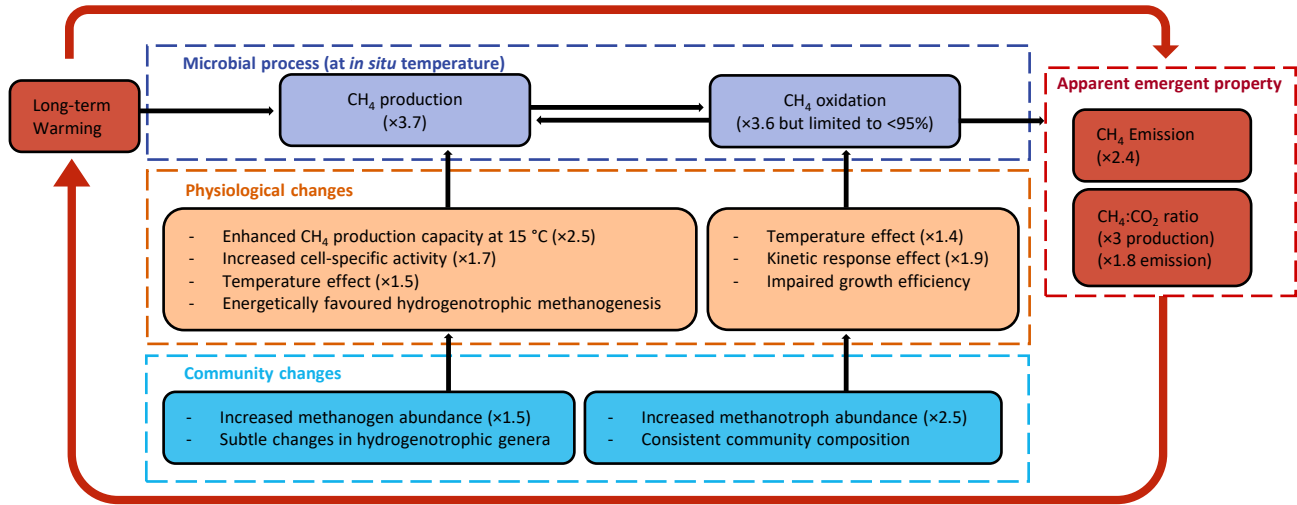


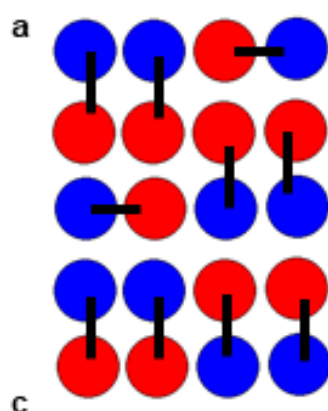
Treatment ○ Ambient ponds ○ Warmed ponds

Rate of oxidation



✗ Predict 1.7-fold increase in CH₄ emission if temperature increases by 4 °C

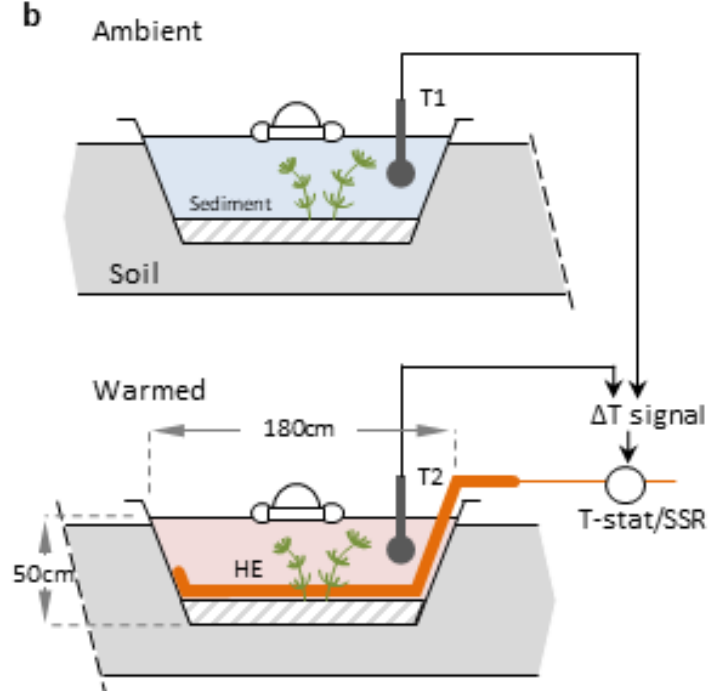




c



b



d

